Characterization and Morphology of TiO₂ Nanocomposites Based on Synthetic and Natural Polymers

Saeed Dadashi, Mehdi Farhoodi, Seyed Mohammad Ali Mousavi, Zahra Emam-Djomeh

Department of Food Science & Technology, Faculty of Agricultural Engineering, University of Tehran, Karaj, Iran P.O.Box: 31587-77871; Telefax: +98 263-224 8804.

Abstract:

Two types of polymers were tested in this study; Poly (Ethylene Terephthalate) (PET) as a synthetic example and Poly (Lactic Acid) (PLA) as a natural polymer. DSC analyses showed that use of nanofiller increases the degree of crystallinity (X_c) of both PET and PLA polymers but the effect was more noticeable on PET nanocomposites. The point of crystallization of PLA and PET nanocomposites occurred at higher temperatures in comparison to neat polymers. Results of the mechanical test showed that for both PET and PLA nanocomposites, the most successful toughening effect was observed at 3 wt% loading of TiO₂ nanoparticles. SEM micrographs revealed uniform distribution of TiO₂ nanoparticles at 1 and 3 wt% loading levels. The results of WAXD spectra explained that crystal type in PLA and PET was not affected by presence of TiO₂ nanoparticles.

Keywords: Nanocomposites; Poly (Lactic Acid); Poly (ethylene terephthalate); Crystallization; Mechanical Properties

INTRODUCTION

Poly(ethylene terephthalate) (PET), produced from ethylene glycol and either terephthalic acid or dimethyl terephthalate, is commonly used as a packaging material for drinking water, mineral water, carbonated beverages and edible oils. The strength and permeability properties of PET; its resistance to chemicals and its high degree of transparency are the main factors that make it superior to most other synthetic polymers. However, the use of synthetic polymers is gradually being replaced by biodegradable materials. Polymers from renewable sources have attracted increasing attention over the last two decades, for two major reasons: firstly, environmental concerns, and secondly the realization that our petroleum resources are finite [1]. Generally, polymers from renewable sources can be classified into three groups: (1) natural polymers such as starch, protein, and cellulose, (2) synthetic polymers from bio-derived monomers such as poly (lactic acid) (PLA); and (3) polymers from microbial fermentation such as poly hydroxy butyrate [2]. In recent years, poly (lactic acid) (PLA) has become increasingly popular as a biodegradable engineering plastic because of its mechanical strength and simple processing compared to other biopolymers [3]. The main limitations of this biodegradable polymer on further industrial application are its poor thermal and mechanical resistance and limited gas barrier properties compared to equivalent petroleum based polymers. These drawbacks limit its access to some industrial sectors, such as packaging, in which its use would be justified when biodegradability is required [4]. Despite abundant use of synthetic and natural polymers, in the past decades polymers reinforced with micrometer fillers have been used to obtain higher strength and stiffness; to improve solvency or fire resistance, or simply to reduce cost. However, the incorporation of these micro sized fillers has some drawbacks such as brittleness and opacity. Nanocomposites, of which at least one dimension of the filler is in the nanometer range, present an alternative approach to overcome the limitations of traditional fillers [5]. Besides, the mentioned properties, improvements in nanocomposites can be achieved at a very low loading of the nanoscale inorganic component (<5wt %), but traditional microcomposites usually require much higher loadings (25-40 wt %) [6]. However, to achieve the mentioned positive effects of nanoparticles on properties, adequate dispersion of nanofillers within the polymeric matrix is required. However, different parameters like polymer type and morphology, type and size of nano fillers, the interaction of nano fillers with the polymeric matrix and its volume content could influence the characteristics of nanocomposites. Among many different types of nano sized fillers, TiO₂ nano powder is increasingly being investigated because it is non-toxic, chemically inert, has broadband UV filter properties, is anti-bacterial from its photo-irradiation effect, corrosion resistant and has high level hardness, high refractive index and low cost [7]. The effects of nano sized TiO₂ on crystallization and the viscoelastic behaviour of synthetic [8-10] and natural [11-13] polymers have been discussed in some other research. Depending on the polymeric matrix type, the addition of TiO₂ nanoparticles could increase [8] or decrease [12, 13] the degree of crystallinity of nanocomposites. Other parameters like melting point, glass transition, and crystallization rate could also change according to polymer structure [14]. The purpose of this study was to investigate the role of polymer type (synthetic or natural) on physical and thermo-mechanical properties of the prepared polymer/TiO₂ nanocomposites. The effects of various levels of nanofiller loading and its dispersion were also investigated.

EXPERIMENTAL PART

Materials

Pure poly (ethylene terephthalate)(PET) (blow molding grade) with intrinsic viscosity of 0.82 dL/g was provided by Tondgooyan Petrochemical Company (Iran). Poly (lactic Acid) (PLA) was purchased from Kunststoff GmbH Siemensring 79 (Germany). Anatase TiO₂ nanoparticles were supplied by Nanoshel LLC (USA). The average diameter of the particles (as recorded by the company) was about 20 nm. Chloroform Solution (analytical-grade) was purchased from AppliChem (Darmstadt, Germany).

1

Preparation of nanocomposites

PLA nanocomposite films were prepared by solution casting. PLA pellets were dried in a vacuum oven at 60°C for 24 h before nanocomposite preparation. 3 and 5 wt% solutions of PLA in chloroform were prepared by stirring the components on a plate at 50°C until the pellets were fully dissolved (8 hr). Nanocomposites containing 3 and 5 wt% nanoparticles (coded as PLA3 and PLA5 in the following text) were prepared by adding nano TiO$_2$ to chloroform solutions with about 95 wt% of PLA pellets dissolved in them. The solutions were then stirred and sonified for 30 min prior to casting. The materials were then cast in Petri dishes greased with silicon and left at room temperature for a week allow the chloroform to evaporate. The prepared films had a thickness of 80 microns. Pure PLA film (coded as PLA0) was prepared in the same way. PET nanocomposites containing 3 and 5 wt% of TiO$_2$ (coded as PET3 and PET5 in the following parts) were prepared via melt blending in a lab-scale counter-rotating twin-screw extruder (Collin ESC-T10 model) with screw diameter of 50 mm and L/D ratio of 15. The extruder has 5 heater zones and a die zone, set at 250, 270, 275, 270, 265, and 265°C and operated at a screw speed of 90 rpm. Nanocomposite components were dried in an oven at 170°C for 5 h before the extrusion process. The prepared profiles were water-cooled and then milled using conventional milling equipment. Neat PET sample (coded as PET0) as reference material was prepared in the same procedure.

DSC *analysis*

The melting and crystallization characteristics of PET and PLA in the prepared samples were studied by a differential scanning calorimeter (DSC 200 F3 Maia® NETZSCH, Germany). The melting behaviour of nanocomposite samples was determined using heating and cooling tests between 25-270 °C for PET and 25-200 °C for PLA at a rate of ±10 °C/min. The first heating run used to erase the thermal history and all data were obtained from the second heating curve of the DSC thermograms. The degree of crystallinity (X$_c$) of polymer in the nanocomposites and neat polymer specimens were calculated using equation (1):

$$X_C = \left(\frac{\Delta H_m}{\Delta H_{m0}} \right) \times 100 \qquad (1)$$

Where ΔH_{m0} is the melting enthalpy of 100% crystalline PET and PLA (ΔH_{m0}=105.97 J/g [8] for PET and 87 J/g [15] for PLA), ΔH_m is the melting enthalpy of the samples.

X-ray diffraction (XRD)

The XRD patterns were recorded in an X-ray diffractometer (Simens D5000-Germany) at room temperature, using Cu Kα tube radiation with the wavelength of 1.5409 oA, generated at 30 kV and 30

mA. The samples were scanned in the range of 2θ = 2–80° with a step size of 0.04o.

Scanning electron microscopy (SEM)

The bulk morphology of the prepared samples was investigated using field emission scanning electron microscopy (FE-SEM; Hitachi S-4160) under an acceleration voltage of 15 kV. The specimens were fractured in liquid nitrogen and the cross surface of samples were coated by gold using a sputtering process.

Tensile testing

Engineering stress-strain curves were prepared from uniaxial tension tests (following ASTM D638) on injection molded dumbbell-like specimens using a Galdabini Sun2500 tensile tester (Galdabini, Italy). The tensile tests were carried out at crosshead speed of 5 mm/min for PET samples and 50 mm/min for PLA samples. At least five specimens for each sample were tested. The mechanical characteristics of each sample were determined in terms of stress at break, strain at break, elastic modulus and dissipated energy.

RESULTS AND DISCUSSION

Morphological observations

SEM micrographs of PET nanocomposites showed that uniform distribution and good dispersion of TiO$_2$ through PET matrix were achieved at 1 and 3 wt%, while at higher loading levels of up to 5 wt%, nanoparticles tended to accumulate (Fig. 1). The average size of a single TiO$_2$ nanoparticle is 20 nm (as mentioned in data sheet of company), however when these nanoparticles agglomerate their size can reach up to to 100 nm (Fig. 1, c-1).

According to Fig. 2 (e), the distribution of TiO$_2$ nanoparticles in PLA1 seems to be uniform with less small sized agglomerates. When the TiO$_2$ loading level raised to 3 wt% there was more of the larger sized agglomerates (more than 300 nm) observed in the polymer matrix (Fig. 2, f). Subsequently at higher loading levels of TiO$_2$ (up to 5 wt%) nanoparticles tendency to agglomerate intensified and more of the larger sized agglomeration is observed (Fig. 2, g). This tendency is stronger for PLA nanocomposites in which agglomeration occurs at lower TiO$_2$ loading. Such agglomeration significantly influences the properties of nanocomposites.
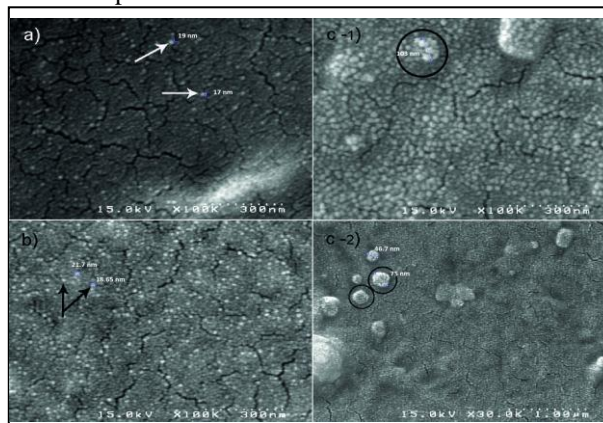

2

Figure 1. SEM micrographs of fracture surfaces of PET-TiO₂ nanocomposites: PET1 (a), PET3 (b) and PET5 (c-1 and c-2), c-2 is
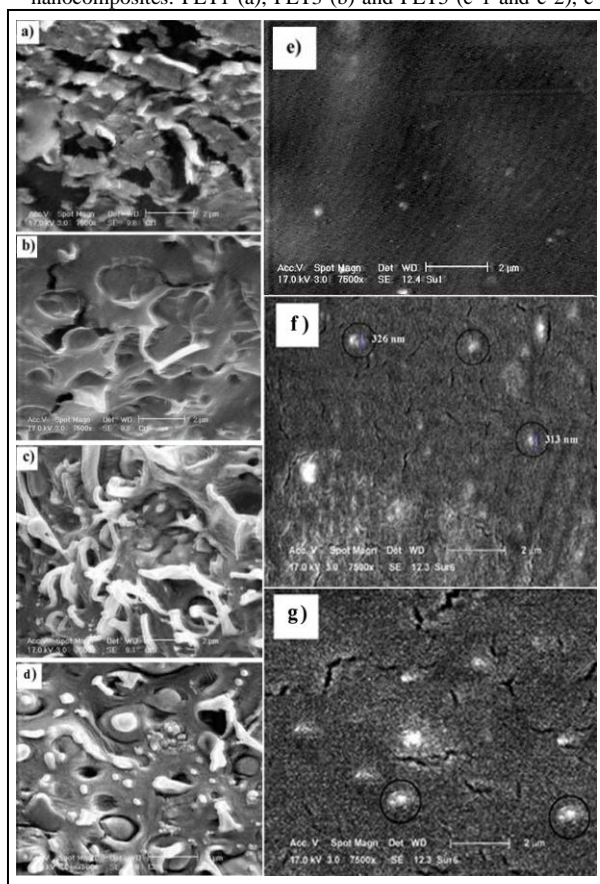

Figure 2. SEM micrographs of fracture surfaces and surface of neat PLA and PLA-TiO₂ nanocomposites: neat PLA (a), PLA1 (b, e), PLA3 (c, f), PLA5 (d, g)

Differential Scanning Calorimetry (DSC)

Values for glass transition temperature (T_g), melting temperature (T_m), crystallization temperature (T_c), enthalpy of melting (ΔH_m), and the degree of crystallinity (X_c) are listed in Tab. 1. T_g of a polymer system varies for a variety of reasons, including changes in tacticity, molecular weight, crosslinking density, free volume, and amount of reaction residue acting as a plasticizer [16]. Tab. 1 shows that the reduction of T_g for PET nanocomposites with increasing TiO₂ content is not very significant. Todorov et al. (2009) observed an unnoticeable effect of TiO₂ nanoparticles on the glass transition point of PET [9].

TABLE 1. THE CHARACTERISTIC VALUES OF DSC ANALYSIS OF DIFFERENT SAMPLES

Sample	T_g (ºC)	T_m (ºC)	T_c (ºC)	ΔT_m (ºC)	ΔH_m (J/g)	X_C (%)
PET0	81.5	249.2	187.5	20.1	35.48	33.48
PET1	80.3	250.0	191.8	22.2	35.02	33.04
PET3	80.7	249.9	193.2	30.1	42.05	39.68
PET5	80.8	250.0	191.8	21.1	34.30	32.36
PLA0	53.83	153.95	84.83	30.14	11.99	13.78
PLA1	52.59	152.19	85.61	30.02	14.01	16.10
PLA3	48.40	153.14	85.47	30.43	12.40	14.94
PLA5	48.54	152.31	86.60	29.87	11.33	12.92

However, in this study, the addition of TiO₂ nanoparticles to the PLA matrix caused a more noticeable reduction of glass transition of PLA, as the glass transition of PLA nanocomposites containing 1, 3 and 5 wt% nanoparticles decreased by 2.3%, 10.1% and 9.8% compared to neat PLA, respectively. Similar results were also found in other researches by Nakayama et al. (2007) and Zhang et al. (2009) [13, 17]. The incorporation of nanoparticles could disturb the packing and regularity of polymer chains and cause free volume increment in a system. This effect could be more significant at higher nanoparticle contents, when more agglomerations form in the matrix. Therefore, the falling level of glass transition in PLA nanocomposites is more noticeable, which could be from the result of a higher amount of TiO₂ agglomerate or non-uniform dispersion of nanoparticles.

Compared to neat PET, the crystallization temperatures (T_c) of PET nanocomposites shift to higher temperatures. Yamada et al. (2006) observed that the PET/TiO₂ nanocomposites containing 0.5, 1 and 2 wt% TiO₂ had higher crystallization temperatures compared to neat polymer [8]. In another research, it was determined that PET/BaSO₄ composites exhibited a higher temperature crystallization point (T_c= 203 °C) than neat PET (T_c=191 °C) [18]. The same trend was observed for PET/SiO₂ composites [19]. These observations could be due to the heterogeneous nucleation effect of nanoparticles' surface on the crystallization of PET macromolecules, which reduces the need for meeting the barrier activation energy of thermal homogeneous nucleation [20]. Therefore, the crystallization process of nanocomposites can begin at higher temperatures than pure polymer. As a result of this phenomena, the nucleation rate and consequently overall crystallization kinetics is promoted. The aforementioned reduction in the crystallization peak width could verify the increment of overall crystallization rate of the prepared nanocomposites. However, the increment in T_c values of PLA nanocomposites is not noticeable. This could be as a consequence of poor dispersion of nanoparticles in these nanocomposites. Second heating curves of pure PET and PLA and their nanocomposites are displayed in Fig. 3. As shown in Fig. 3, the melting points of PET nanocomposites show negligible changes comparing to the PET0 sample. However, for PLA nanocomposites, a decrease in T_m is observable especially in the case of PLA5. For PET3, the melting peak is broader (ΔT_m =30.1ºC compared to 20.1ºC for PET0). This result is a direct consequence of broader crystallite size distribution in the presence of solid nanoparticles that could induce imperfections during the crystallite growth process. Thus, various sizes of the formed crystallites in nanocomposites with different thermal stabilities broaden the melting peaks. A comparison of the ΔT_m of different nanocomposites to that of pure polymers shows that this phenomenon could occur for nanocomposites with good dispersion and distribution of nanoparticles, while for nanocomposites with higher
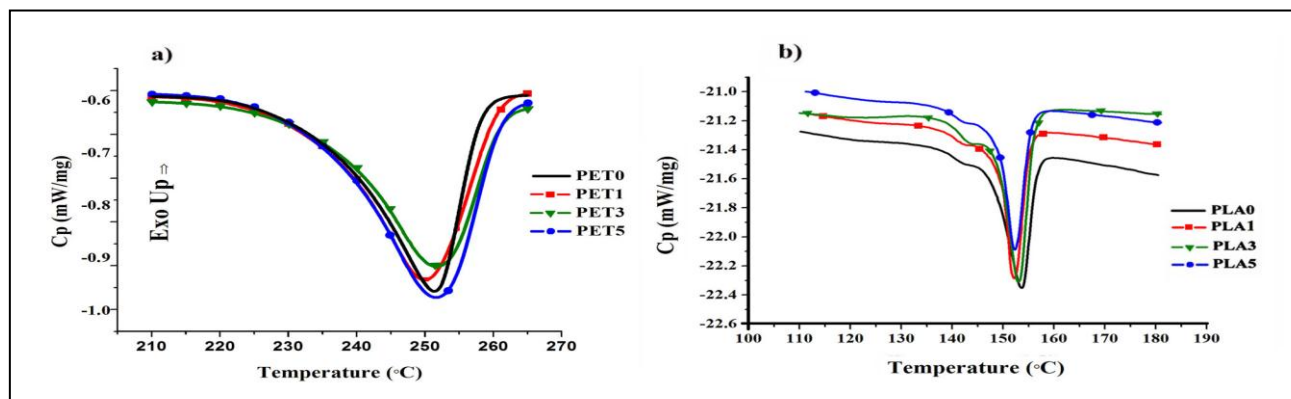
3

Figure 3. Second heating curves of the prepared PET (a) and PLA (b) samples

amounts of agglomeration the opposite action occurs (PLA3 and PLA5). Another characteristic value of the crystallization process is the final degree of crystallinity, shown in Tab. 1 for different prepared samples. Compared to neat PET, the sample containing 3 wt% TiO_2 has the highest X_c. As demonstrated, X_c of the prepared nanocomposites show an optimum value with an increasing nanoparticle loading. However, when the content of TiO_2 in PET matrix increases to 5 wt%, X_c tends to decrease, suggesting high nanofiller content significantly restricts the mobility of polymer chain segments. Another important effect of the incorporation of nanofiller in to polymers and their crystallization process is that nanoparticles can create a physical hindrance to the motion of polymer chains. Thus, the nano filler's surface and nanoparticle agglomerates could limit crystal growth, resulting in a decrease of X_c and the degree of crystallite perfection. Fig. 1 shows that at lower concentrations of nanofiller (PET1 and PET3), uniform distribution and appropriate dispersion of TiO_2 nanoparticles through matrix was obtained. While, increasing the TiO_2 loading up to 5 wt% leads to nanoparticle agglomeration. Therefore, the interaction of polymer chains with higher accessible solid surfaces and embedding of a portion of macromolecule chain length in nanofiller agglomerates could significantly hinder the segmental motion of polymer chains during crystallization. This phenomenon could be the reason that the PET5 sample showed lower X_c.

Reduction of X_c and melting point in PLA nanocomposites has been reported in other research [17, 21]. Zhang, et al. (2009) suggested that the reason for these phenomena is probably the efficient role of TiO_2 nanoparticles in disarranging the regularity of chain structures of PLA and increasing spaces between the chains [17]. While, Liao, et al. (2012) stated that the lower melting temperature and crystallinity of PLA nanocomposite is due to an increment in the number of small crystallites and subsequently lower overall crystallinity of PLA in the presence of nanoparticles [21]. In this research, it seems that disarranging of PLA chains occurs at higher loading levels of TiO_2 nanoparticles as showed in Fig. 2 with bigger agglomeration size (PLA3 and PLA5 as shown in Fig. 2) while at 1% loading level, relatively uniform dispersion of nanoparticles results in increased crystallinity due to the nucleation effect of

nanoparticles. Generally, the crystallization behaviour of nanocomposites depends on the nanofiller loading, its dispersion in the matrix and the type of matrix. Crystallization is determined by the relative dominating status of two different effects of nanoparticles on the crystallization process i.e. the nucleation effect and the growth restriction effect. At low level TiO_2 content and uniform dispersion of nanoparticles, the first effect dominates. Therefore, there is a high value X_c of PET3 and PLA1 samples. However, increasing the nanofiller loading and agglomerate formation could alter the situation in which the hindrance of macromolecule motion becomes stronger. Nucleation effects of TiO_2 nanoparticles on crystallization behaviour of PET matrix seem much stronger than on the PLA matrix.

Tensile testing

The mechanical properties of neat polymers and prepared nanocomposites were listed in Tab. 2. It was expected that the elastic modulus of nanocomposites would increase with the addition of mineral rigid nanoparticles, but results collected in Tab. 2 show that there is not a significant difference in the magnitude of modulus of nanocomposites from that of pure polymers. Large standard deviation of the modulus values causes an overlap in the results of different samples.

As demonstrated, the tensile strength of nanocomposites decreased compared with that of neat polymer. This could be attributed to the preventative effect of nanoparticles on strain hardening of the polymer chains after cold drawing. This strain hardening phenomenon plays a critical role in stabilizing polymers against strain localization, fracture and reducing wear [25]. So, it can be determined that nanofiller, as heterogeneous solid nanoparticles, could hinder polymer stress induced crystallization and subsequently decrease resistance of the polymer network against fracture. Another attractive effect of the addition of nanoparticles on mechanical properties is the increment of strain at break and dissipated energy or ductility (lost energy determined from the area under the stress-strain curve up to break). In the other words, the nanocomposite ductility enhanced with an addition of TiO_2 nanofiller. Incorporation of TiO_2 nanoparticles in to the PET matrix increased the strain at break of PET1, PET3 and PET5 nanocomposites by 313, 444 and 192%, respectively. Also the strain at break of PLA1, PLA3 and PLA5 nanocomposites comparing to

4

TABLE 2. MECHANICAL PROPERTIES OF NEAT PET, NEAT PLA AND THEIR

Sample	Stress at break (MPa)	Strain at break (%)	Elastic modulus (MPa)	Dissipated energy (J)
PET0	59.6 ± 2.9	5.2 ±1.6	2467.2 ± 198.5	3.8 ± 0.6
PET1	28.3 ± 6.5	21.5 ± 4.5	2486.1 ± 96.5	4.7 ± 1.7
PET3	30.7 ± 2.0	28.3 ± 3.4	2561.3 ± 191.7	9.4 ± 2.3
PET5	36.9 ± 5.8	15.3 ± 2.6	2572.8 ± 103.2	7.1 ± 1.3
PLA0	27.44 ± 2.75	24.53 ± 1.60	1840 ± 110	3.78 ± 0.21
PLA1	26.33 ± 3.54	29.86 ± 2.33	1710 ± 140	3.85 ± 0.24
PLA3	25.14 ± 4.23	38.50 ± 3.42	1780 ± 150	5.25 ± 0.35
PLA5	23.47 ± 2.54	35.82 ± 2.64	1660 ± 170	4.42 ± 0.28

neat PLA increased by 22, 57 and 46%, respectively. This effect could be as a consequence of the creation of new energy damping mechanisms in the presence of nanoparticles such as the breaking up of agglomerates, void nucleation, crack deflection, nanofiller debonding or pull out, matrix deformation and bridging. During occurrence of the first two mechanisms, particle agglomerates are broken up and debonded from the matrix, creating smaller or larger voids. The breaking up or debonding stress determines the crazing stress, which is lower than that in an unfilled matrix. Therefore, slight agglomeration facilitates crazing and more crazes can be created with a positive effect on energy dissipation and toughness [26]. However, as observed in Tab. 2, the levels of dissipated energy of PET5 and PLA5 decreased compared to those of PET3 and PLA3 samples, respectively. As the nanoparticle size increases and large agglomerates are formed, the total particle/matrix interfacial surface area available for energy dissipation decreases, but the critical stress for particle/matrix debonding also decreases and this could be the reason for observation of an optimum level of ductility with increasing nanoparticle loading. In similar research, it was found that incorporation of TiO_2 to PET could cause an increase of elongation at break [9]. The maximum toughening effect of nanoparticles in the PLA3 sample shows the highest amount of dissipated energy in tensile tests, confirmed by DMTA results. The micrographs obtained by SEM also verify these results (Fig. 2, a-d). At 3 wt% loading of TiO_2 in PLA, the crazes at sample surface reach its minimum level and an increased toughening effect is observed on the fracture surface (Fig 2, c). Energy dissipation and reinforcement mechanisms work well only if a special state of particle dispersion is reached. As demonstrated, in nanocomposites containing 3 wt% of TiO_2 in which more homogenous dispersion of nanoparticles is achieved, the dissipation and reinforcement mechanisms are more active. When nanoparticles have an optimum distance from each other and are uniformly dispersed in a matrix, there is a transition from brittle failure (in the neat polymer) towards tough failure behaviour (in nanocomposites).

X-ray diffraction
To investigate the influence of TiO_2 nanoparticles on the crystalline structure, WAXD spectra of pure TiO_2, the neat polymers and the prepared nanocomposites

were obtained. The results are shown in Fig. 4. The incorporation of nanoparticles to pure polymers and increasing its loading causes no shift in the peak position of crystalline planes of PET and PLA verifying that the type of crystals do not alter in the presence of TiO_2. As demonstrated, by considering peak intensities, PET3 and PLA1 samples show a higher content of crystalline structure compared to pure polymers. While for nanocomposites including higher loading of nanoparticles, peak intensities reduce. These consequences confirm the results of DSC analysis, in that the highest degrees of crystallinity are obtained in PET and PLA nanocomposites with 3 and 1 wt% TiO_2, respectively. At these contents, the role of nanoparticles in the creation of heterogeneous nucleation sites is dominated. The crystalline peaks of TiO_2 powder also can be observed in different nanocomposites' spectra and the intensities are related to the content of nanoparticles in these samples.
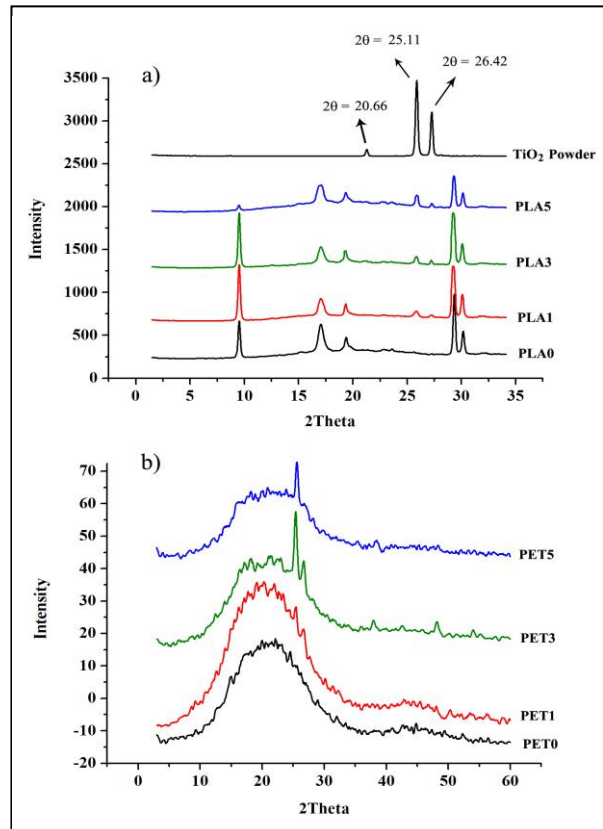

Figure 4. WAXD spectra of anatase TiO_2, neat PLA and PLA nanocomposites (a), neat PET and its nanocomposites (b)

5

CONCLUSIONS

Results of the DSC analysis showed that the crystallization temperatures of PET and PLA nanocomposites was higher with increasing TiO_2 loading in the polymer matrix and that the percentage of crystallinity first increases and then decreases with incremental additions of TiO_2. Degrees of crystallinity in PLA and PET nanocomposites reach maximum values in nanocomposites containing 1 and 3 wt% nanoparticles, respectively, but this effect is more evident in PET nanocomposites. These results demonstrate that an addition of TiO_2 could significantly enhance the rate of PET crystallization as a result of heterogeneous nucleation effect of TiO_2. Morphological observations show that nanoparticle dispersion is more homogenous in a PET matrix than in a PLA matrix. The results of the tensile test show that elongation at break and dissipated energy increase with additions of TiO_2 nanoparticles into PET and PLA matrices that reach the maximum amount at 3% loading level of TiO_2. These improvements of ductility could be as a result of new damping mechanisms that are more active in homogenous dispersion and distribution of nanoparticles. The XRD patterns show that incorporation of nanoparticles to the pure matrices and increasing its loading cause no shift in the peak position of crystalline planes. According to UV-Visible spectra, both PET and PLA nanocomposite films exhibited high UV shielding, with transparency loss.

REFERENCES

[1] L. Yu, K. Dean, and L. Li, "Polymer blends and composites from renewable resources," Progress in Polymer Science, 31(6), 576, 2006.

[2] L. Yu, and L. Chen, "Polymeric materials from renewable resources. Biodegradable polymer blends and composites from renewable resources," John Wiley & Sons Inc., pp. 1-15, 2009.

[3] J. Lunt, "Large-scale production, properties and commercial applications of polylactic acid polymers," Polymer Degradation and Stability, 59, 145, 1998.

[4] R. P. Singh, J. K. Pandey, D. Rutot, Ph. Degee, and Ph. Dubois, "Biodegradation of poly (o-caprolactone)/starch blends and composites in composting and culture environments: the effect of compatibilization on the inherent biodegradability of the host polymer," Carbohydrate Research, 338, 1759, 2003.

[5] M. Rosoff, "Nano-surface Chemistry," Marcel Dekker Inc., New York, 2002.

[6] C. Saujanya, and S. Radhakrishnan, "Structure development and crystallization behaviour of PP/nanoparticulate composite," Polymer, 42, 6723, 2001.

[7] D. H. Solomon, and D. G. Hawthorne, "Chemistry of Pigments and Fillers," John Wiley & Sons Inc., New York, 1983.

[8] T. Yamada, L. Hao, K. Tada, S. Konagaya, and G. Li, "Crystallization characteristics of Pet/TiO_2 nanocomposites," Material Science, 2, 154, 2006.

[9] L. V. Todorov, C. I. Martins, and J. C. Viana, "Characterization of PET nanocomposites with different nanofillers," Solid State Phenomena, 151, 113, 2009.

[10] L. V. Todorov, and J. C. Viana, "Characterization of PET nanocomposites produced by different melt-based production methods," Journal of Applied Polymer Science, 106, 1659, 2007.

[11] L. Yonghui, Ch. Caihong, L. Jun, and S. S. Xiuzhi, "Synthesis and characterization of bionanocomposites of poly (lactic acid) and TiO_2 nanowires by in situ polymerization," Polymer, 52, 2367, 2011.

[12] L. Xili, L. Xiuqian, S. Zhijie, and Zh. Yufeng, "Nanocomposites of poly (l-lactide) and surface-grafted TiO_2 nanoparticles: Synthesis and characterization," European Polymer Journal, 44, 2476, 2008.

[13] N. Nakayama, and T. Hayashi, "Preparation and characterization of poly (l-lactic acid)/TiO_2 nanoparticle nanocomposite films with high transparency and efficient photodegradability," Polymer Degradation and Stability, 92, 1255, 2007.

[14] J. W. Rhim, S. I. Hong, and C. S. Ha, "Tensile, water vapor barrier and antimicrobial properties of PLA/nanoclay composite films," LWT- Food Science and Technology, 42, 612, 2009.

[15] E. W. Fisher, H. J. Sterzel, and G. Wegner, Kolloid-Zeitschrift and Zeitschrift Fur Polymere, 251 (11), 980, 1973.

[16] Y. Y. Sun, Z. Q. Zhang, K. S. Moon, and C. P. Wong, "Glass transition and relaxation behavior of epoxy nanocomposites," Journal of Applied Polymer Science, 42 (21), 3849, 2004.

[17] Y. C. Zhang, J. N. Huang, H. Y. Wu, and Y. P. Qiu, "Effect of TiO_2 nanoparticle on thermal and tensile behavior of polypropylene/polylactic acid composite," Materials Science, 613, 316, 2009.

[18] M. H. Qu, Y. Z. Wang, C. Wang, X. G. Ge, D. Y. Wang, and Q. Zhou, "A novel method for preparing poly(ethylene terephthalate)/BaSO4 nanocomposites," European Polymer Journal, 41, 2569, 2005.

[19] J. P. He, H. M. Li, X. Y. Wang, and Y. Gao, "In situ preparation of poly (ethylene terephthalate)–SiO_2 nanocomposites," European Polymer Journal, 42 (5), 1128 2006.

[20] T. Wan, L. Chen, Y. C. Chua, and X. Lu, "Crystalline morphology and isothermal crystallization kinetics of poly (ethylene terephthalate)/clay nanocomposites," Journal of Applied Polymer Science, 94, 1381, 2004.

[21] X. Liao, A. Nawaby, and H. E. Naguib, "Porous poly (lactic acid) and PLA-nanocomposite structures," Journal of Applied Polymer Science, 124 (1), 585, 2012.

[22] S. Pattanawanidchai, P. Saeoui, and C. Sirisinha, "Influence of precipitated silica on dynamic mechanical properties and resistance to oil and thermal aging in CPE/NR blends," Journal of Applied Polymer Science, 96, 2218, 2005.

[23] P. C. Chiang, W. T. Whang, and M. H. Tsai, "Physical and mechanical properties of polyimide/titania hybrid films," Thin Soild Films, 447, 359, 2004.

[24] M. H. Tsai, S. J. Liu, and P. C. Chiang, "Synthesis and characteristics of polyimide/titania nano hybrid films," Thin Solid Films, 515, 1126, 2006.

[25] Y. J. Mergler, and R. P. Schaake, "Relation between strain hardening and wear resistance of polymers," Journal of Applied Polymer Science, 92, 2689, 2004.

[26] L. Sun, R. F. Gibson, F. Godaninejad, J. Suhr, "Energy absorption capability of nanocomposites: a review," Composite Science and Technology, 69, 2392, 2009.

[27] C. Espejo, A. Arribas, F. Monzo, and P.P. Diez, "Nanocomposite films with enhanced radiometric properties for greenhouse covering applications," Journal of plastic film and sheeting, 1-16, 2012.

6